



# ASSESSMENT OF PHOTO LUMINESCENCE BEHAVIOUR OF SPRAY PYROLYSED ZnAl<sub>2</sub>O<sub>4</sub> THIN FILMS SUITABLE FOR LIGHT EMITTING DIODE APPLICATION

J. Merrila Nissi<sup>1</sup>, T.R. Beena<sup>1</sup>, R. Shabu<sup>2</sup>

<sup>1</sup>Research Scholar (Reg. No: 19213162132018), Department of Physics and Research Centre,  
Scott Christian College (Autonomous), Nagercoil - 629 003, Tamil Nadu

<sup>2</sup>Department of Physics, St Alphonsa College of Arts and Science, Karungal-629157,  
Tamil Nadu

<sup>1</sup>Affiliated to Manomaniam Sundaranar University, Tirunelveli - 627 012, Tamil Nadu

## Abstract

Zinc Aluminate (ZnAl<sub>2</sub>O<sub>4</sub>) thin films have been deposited on glass substrates using chemical spray pyrolysis technique by varying the substrate temperature from 350 °C to 450 °C (in steps of 50 °C). The effect of substrate temperature on the structural, optical, morphological, and luminescence properties of the obtained films have been investigated. Films which were characterized had a thickness of the order of a few micrometers. The XRD pattern reveals that the synthesized films are preferentially oriented along the (311) plane. Optical transmittance for these films is maximum along the (NIR) near-infrared region and visible region. Moreover, these films possessed band gap energy in the range of 3.84-3.90 eV. SEM images confirm the presence of spherical-shaped particles with a porous crystalline structure. From the Photo Luminescence spectrum, it is observed that the film deposited at 400 °C exhibited the highest peak intensity for all observed emission bands. Zinc Aluminate (ZnAl<sub>2</sub>O<sub>4</sub>) films show emission bands at 483 nm (blue), and 663 nm (red) under 350 nm and 244 nm excitation respectively. The emission spectral data were used to compute yellow/blue ratios, colour chromaticity coordinates (x, y), and correlated colour temperatures (CCT). The obtained CIE Values were found to be in good agreement with the blue region (0.14, 0.08) and red region (0.67, 0.33) respectively under different excitations. This observation confirmed that the prepared thin films excited at 224 nm and 350 nm emitted warm and cool daylight which are suitable for blue light applications and laser applications.

## 1. Introduction

Persistent luminescence materials frequently consist of an inorganic matrix (known as a host) and activated doping ions (activator). In these materials, luminescence emission can be generated by an optical center (luminescence center), charge transfer, or optical transitions between host lattice-related band states. In recent years, spinel-type materials are interesting

research topics because they have properties like high chemical, thermal stability, and mechanical resistance [1, 2]. Zinc Aluminate is a well-known wide band gap material ( $E_g=3.8eV$ ) with a spinel structure  $AB_2O_4$  which belongs to a space group of  $Fd-3m$ . Here A stands for a metal cation that occupies a tetrahedral site and B stands for a metal anion that occupies the octahedral site of a cubic-packed structure [3]. To our knowledge, Zinc Aluminate has attracted much attention because of its physical and chemical properties. They are widely used in many applications such as optoelectronic devices [4], gas sensors [5, 6], electronics and photocatalysts [7].  $ZnAl_2O_4$  oxides show the migration of photo generated carriers, thereby providing the separation efficiency of photo generated pairs across the heterojunction by injecting electrons into the lower-lying conduction band of the large band gap semiconductor [8,9]. Kumar et al. reported that the presence of high surface area and thermal stability of the  $ZnAl_2O_4$  oxides helps to suppress the recombination of photo generated electrons and holes.

Based on the above-mentioned applications, various morphologies of spinel  $ZnAl_2O_4$  have been prepared [10-14]. Nevertheless, the optical properties of the materials mainly depend upon their morphologies and preparation methods. Even though many preparation methods such as the Sol-gel method [16], Solid state reaction method, Co-precipitation method [15], Pulsed laser deposition method [17], and Chemical Vapor deposition method are available for thin film preparations. Chemical Spraypyrolysis technique is being considered in the present study because of its simplicity, cost-effectiveness and for prepared doped samples of any composition.

Currently, researchers put more effort into the production of high-quality phosphors for white light-emitting applications in the phosphor material synthesis research around the world because of the great demand for the light-emitting diode in the market and possible applications in households. However, the PL spectra of  $ZnAl_2O_4$  show strong emission in the visible region which is associated with the defect states in the nanostructures. When transitions occur through defect states, light emission takes place in the visible region and transitions from different defect states result in emission at different wavelengths. There are reports on the green, red and blue [18] emissions in  $ZnAl_2O_4$  films. However, the intensity of emission should be very strong to consider them for the device applications. This was the initiative to work on this material by Chemical Spraypyrolysis method.

## 2. Synthesis and characterizations

### 2.1 Chemicals/Materials

Aluminium Nitrate [ $Al(NO_3)_3 \cdot 9H_2O$ ], Zinc Nitrate [ $Zn(NO_3)_2 \cdot 6H_2O$ ], Ethanol, Deionized water, and Hydrochloric acid(HCl) were used for the sample synthesis. These chemicals were purchased from Sigma Aldrich and used as such without further purification.

### 2.2 Synthesis

In the present study,  $ZnAl_2O_4$  films were deposited by Spraypyrolysis technique by atomizing liquid precursor and further condensation by thermal decomposition on substrates maintained at different temperatures. Zinc nitrate hexahydrate (0.1 M) and Aluminium Nitrate hexahydrate (0.2 M) were used as starting precursors and dissolved in water-ethanol solution in a ratio of 2:1. Prepared precursors were stirred continuously using a magnetic stirrer for 20 minutes to get a clear homogenous solution. Before deposition, the glass substrate was cleaned to get well-adherent and smooth films. At the time of deposition, the distance between the spray nozzle and the substrate was maintained at 30 cm. Spray solution of 50 ml was atomized at the rate of 10 ml/min using compressed air. The substrate temperature was varied from 350 °C to 450 °C and was monitored by an electronic temperature controller.

### 2.3 Characterization

The thickness and roughness of the thin films synthesized were measured using Stylus Profiler. X-ray diffraction (PANalytical/ X Pert3) was used to confirm the crystal structure of the  $ZnAl_2O_4$  films. The optical studies were performed using the double-beam UV-Vis-NIR spectrophotometer in the 300-700 nm wavelength range. High-resolution scanning electron microscopy was used to analyze the surface morphology of the films. The emission bands of the prepared film were investigated using the spectrofluorophotometer (SHIMADZU/ RF 6000).

## 3. Results and Discussion

### 3.1 Thickness

The films ( $ZnAl_2O_4$ ) deposited at different substrate temperatures (350 °C, 400 °C and 450 °C) have a thickness of 5.35  $\mu m$ , 325  $\mu m$ , and 2.25  $\mu m$  respectively. The thickness of the film is found to be decreased considerably with an increase in substrate temperatures from

350 to 450 °C. This may be due to the significant reduction of mass transport to the substrate, due to high temperature. The high deposition temperature also causes the reduction of nucleation over the glass plate. Further, the film deposited at a low temperature (350 °C) shows thick and foggy in nature and the film deposited at a high temperature (400 °C) became highly transparent in nature.

### 3.2 Structural analysis

The influence of deposition temperatures on the structural properties of the synthesized ZnAl<sub>2</sub>O<sub>4</sub> films was studied using X-Ray diffraction. The XRD patterns of ZnAl<sub>2</sub>O<sub>4</sub> thin films deposited at various temperatures are shown in Fig.1.

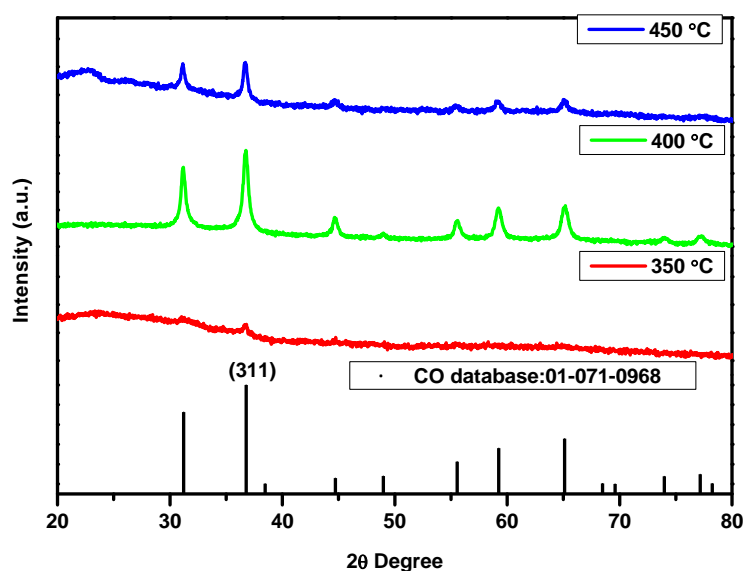


**Fig. 1. XRD patterns of ZnAl<sub>2</sub>O<sub>4</sub> films prepared at various substrate temperatures**

From the XRD pattern it is observed that the deposited ZnAl<sub>2</sub>O<sub>4</sub> films have cubic structure and the diffraction peaks were indexed by comparing the data with the COD database: 01-071-0968.

The absence of extra peaks showed that the deposited films are pure and single phase. The diffraction peaks obtained at  $2\theta = 31.255^\circ$ ,  $36.827^\circ$ ,  $44.786^\circ$ ,  $55.625^\circ$ ,  $59.324^\circ$ ,  $65.198^\circ$ , and  $77.295^\circ$  perfectly matched with the standard (h k l) planes corresponding to (2 2 0), (3 1 1), (4 0 0), (4 2 2), (5 1 1), (4 4 0) and (5 3 3) respectively with preferred orientation along the (3 1 1) plane.

A small peak located at  $2\theta = 36.6679^\circ$  in the film deposited at 350 °C, oriented along (3 1 1) plane was less intense and was amorphous in nature. This is because at low

temperatures the kinetic energy is not enough to stimulate the growth rate process during Spraypyrolysis [19, 20].

At a substrate temperature of 400 °C, the adsorbed radicals got sufficient kinetic energy and hence there was a better accommodation of particles on the deposited film and thus exhibited a highly crystalline nature.

In converse, the film deposited at 450 °C was less crystalline and this may be due to the reaction saturation effect and re-evaporation of the atomic species during the flight from the nozzle to the substrate.

The structural parameters such as lattice constant, unit cell volume, density, and stress were calculated from the peak obtained for the (3 1 1) plane and given in Table 1.

**Table 1 Crystallographic Properties of ZnAl<sub>2</sub>O<sub>4</sub>**

Deposition Temperature (°C)	Lattice Constant (a) (Å)		Unit Cell Volume (Å <sup>3</sup> )		Density ρ (gm/cm <sup>3</sup> )		Stress σ (MPa)
	Cal.	Std.	Cal.	Std.	Cal.	Std.	
350	8.1011	8.0980	531.65	535.05	4.88	4.59	0.100
400	8.1001		535.10		4.60		0.1043
450	8.1126		538.68		4.91		0.1572

The lattice constant values for all the synthesized ZnAl<sub>2</sub>O<sub>4</sub> films are found to exceed the bulk value  $a = 8.0980 \text{ \AA}$ . Moreover, the film deposited at 400 °C showed a minimum lattice constant value which is in close agreement with the standard value.

The stress value of synthesized ZnAl<sub>2</sub>O<sub>4</sub> film was calculated from the relation [21],

$$1 + \frac{\nu}{2E} \sigma^{XRD} = \frac{d-d_0}{d_0} \quad (1)$$

Where E is Young's modulus (193 GPa),  $\nu$  is the Poisson coefficient (0.3241), d is the calculated d-spacing value from the XRD data, and  $d_0$  is the standard d-spacing value from the given CO database.

The obtained film showed good tensile stress whereas high deposition temperature caused compressive stress on the film, and hence nanocrystalline particles were deposited in a fine manner. The synthesized ZnAl<sub>2</sub>O<sub>4</sub> film showed an expansion in unit cell volume that led to an increase in interplanar distance than the

standard value. This causes a strain on the film. Also, the stress in the synthesized film was compressive as reported [22].

Owing to the presence of stress, there could be a strain, and the associated lattice defects. These are calculated by measuring the FWHM from the XRD pattern for the preferentially oriented (3 1 1) plane. The strain and associated lattice defects such as dislocation density and stacking fault probability of each film deposited at different substrate temperatures are listed in Table.2

**Table 2 Measured grain size, microstrain, Dislocation density and stacking fault probability of ZnAl<sub>2</sub>O<sub>4</sub> films deposited at different substrate temperatures**

Deposition Temperature (°C)	(311) interplanar distance, d(Å)	Grain Size, D(nm)	Microstrain, $\epsilon$ ( $\times 10^{-3}$ )	Dislocation density, $\delta$ ( $\times 10^{15}$ lines/cm <sup>-2</sup> )	Stacking fault probability
350	2.8734	20	2.47	2.87	0.05
400	2.8735	21	1.71	2.24	0.04
450	2.8736	24	1.48	1.01	0.03

The lattice defects like microstrain, dislocation density and stacking fault probability showed a decreasing trend with the increase in the substrate temperature. Even though the film thickness decreased with increasing substrate temperature, the crystalline size increased. The reason for this effect is that the migration of grain boundaries caused agglomeration of crystallites and thus bigger crystallites are formed at higher deposition temperatures [22, 23,24]. Therefore, the microstrain, dislocation density, and stacking fault probability decreased due to the lattice imperfections in crystalline materials.

### 3.3 Optical Properties

Zinc Aluminate (ZnAl<sub>2</sub>O<sub>4</sub>) thin films prepared at different substrate temperatures were subjected to optical characterization using UV-VIS-NIR spectra. The optical transmittance spectra of the deposited ZnAl<sub>2</sub>O<sub>4</sub> films were recorded within the range of 300-800 nm spectral regions. From the transmittance data, optical absorption coefficient, optical band gap energy, refractive index (n), and extinction coefficient were calculated. Fig.2 showed the optical transmittance spectra (T %) of ZnAl<sub>2</sub>O<sub>4</sub> films deposited at various substrate temperatures.

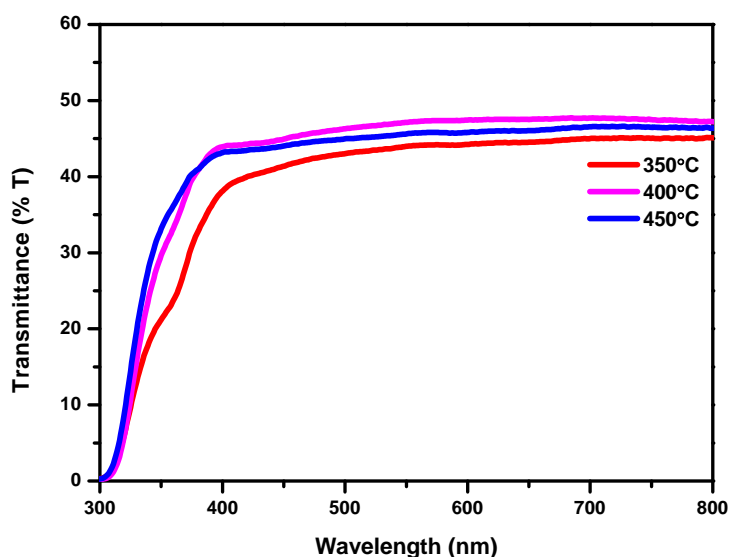


**Fig.2. Optical transmittance spectra of  $ZnAl_2O_4$  films prepared using different substrate temperatures**

The transmittance is found to be maximum for  $ZnAl_2O_4$  film prepared at the substrate temperature 400 °C, due to the well-adherent and highly crystalline nature of the film which was also confirmed by the XRD results. This maximum transmittance may lead to an improvement in the energy and mobility gained by the atoms. Further films deposited at low temperatures exhibited less transmittance due to the foggy nature which has been reported earlier [25]. The optical band gap energy ( $E_g$ ) of  $ZnAl_2O_4$  films was calculated using Tauc's formula,

$$\alpha h\nu = A(h\nu - E_g)^{\frac{1}{n}} \quad (3)$$

The plot of  $(\alpha h\nu)^2$  Vs  $h\nu$  for the  $ZnAl_2O_4$  films deposited at different temperatures is shown in Fig.3

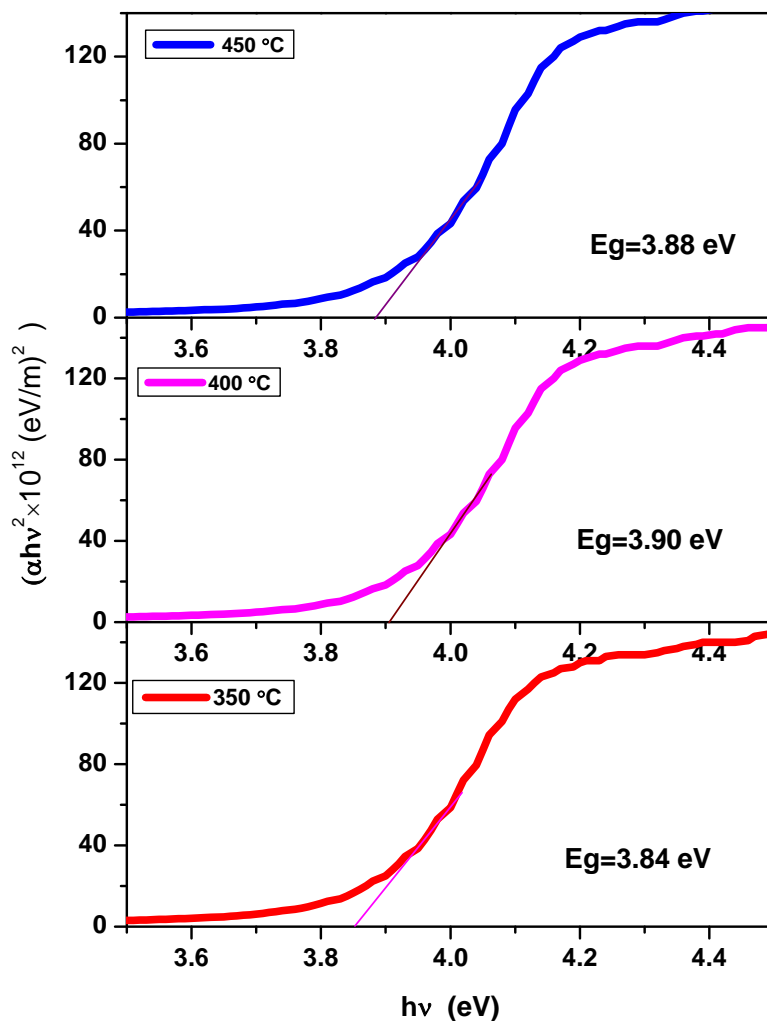


**Fig.3. Tauc's plot of ZnAl<sub>2</sub>O<sub>4</sub> film deposited at various temperatures**

ZnAl<sub>2</sub>O<sub>4</sub> thin films deposited at different substrate temperatures gave the direct allowed band gap values which are varied as 3.84 eV, 3.9 eV and 3.88 eV for the films deposited at 350 °C, 400 °C and 450 °C respectively. This was in close agreement with the results reported earlier [26]. The high band gap value of the film deposited at 400 °C confirmed an increased carrier effect and compression stress [25, 27]. A blue shift occurred due to the quantum confinement that decreased the coordination number and atomic interaction. Hence band gap energy level between VB and CB has increased further.

Fig.4 reveals the variation of the extinction coefficient against wavelength (nm). From the graph, it is observed that the extinction coefficient values are maximum in the lower wavelength region and decreased in the higher wavelength. The peak showed a steep



decrease in the visible region and became parallel to the wavelength axis for the UV region. This change in the value of extinction coefficient was due to the absorption of light along the boundary region [28].

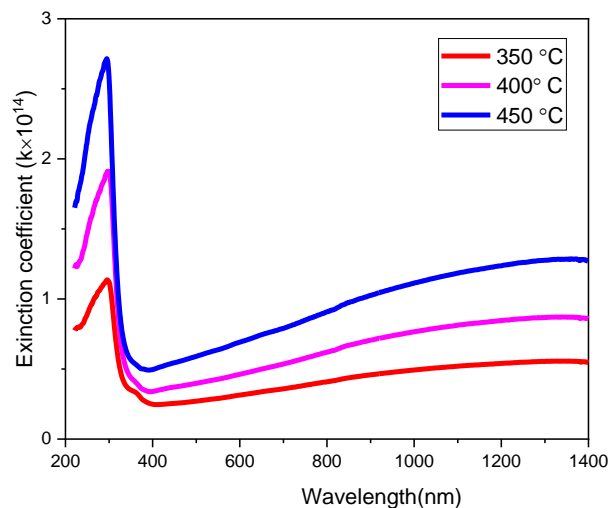


**Fig.4. Variations of extinction coefficient as a function of wavelength**

From fig.5 shows the variation of refractive index with wavelength and it was found to decrease with an increase in wavelength in the UV region and became constant in the visible and IR region. The refractive index values for the deposited thin films at different substrate temperatures such as 350 °C, 400 °C and 450 °C are found to be 2.17, 2.78 and 3.13 respectively in the band edge region. These refractive index values are found to increase with an increase in temperature. This is because as the incident light interacted with a material containing highly dense packed particles, the amount of refraction was high and hence the refractive index of the film increased [29].

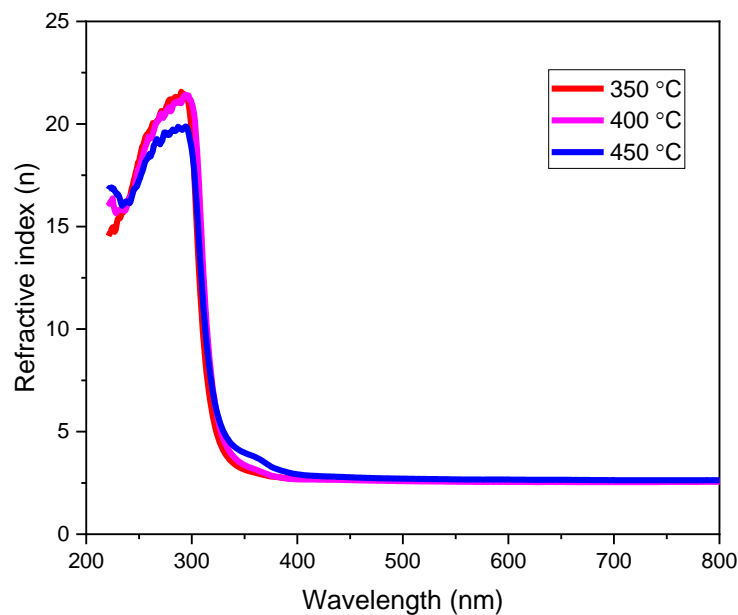


**Fig.5. Refractive index variation with wavelength of  $ZnAl_2O_4$  thin films**

### 3.4 SEM Analysis

Fig. 6 shows the SEM images of  $ZnAl_2O_4$  thin films prepared at various substrate temperatures. SEM images indicated that the particles are spherical in shape with uneven distribution. This is because the film deposited at 350 °C showed grains of spherical shape and their distribution is uneven. For this reason, the grains are agglomerated to give a rough surface. For the optimized film at 400 °C continuous coalescence of particles took place with the formation of film channels between them. At low deposition temperatures, some of the droplets got evaporated and decomposed due to insufficient temperature. At the impact point, droplet vaporization requires some heat that tends to decrease the substrate temperature and directly affects the reaction kinematics which inhibited weak sticking probability. Sometimes these channels may not be completely filled up even with decreasing film thickness thus leaving some holes or gaps in the aggregate mass. Therefore, re-nucleation has taken place at the surface of the previously grown grains and thus each vertical column grows multigranularly. Moreover, the film deposited at 450 °C revealed the growth of bigger grains with clusters of overgrowth. They interlocked with each other and thus became aggregated [19, 20, 30].

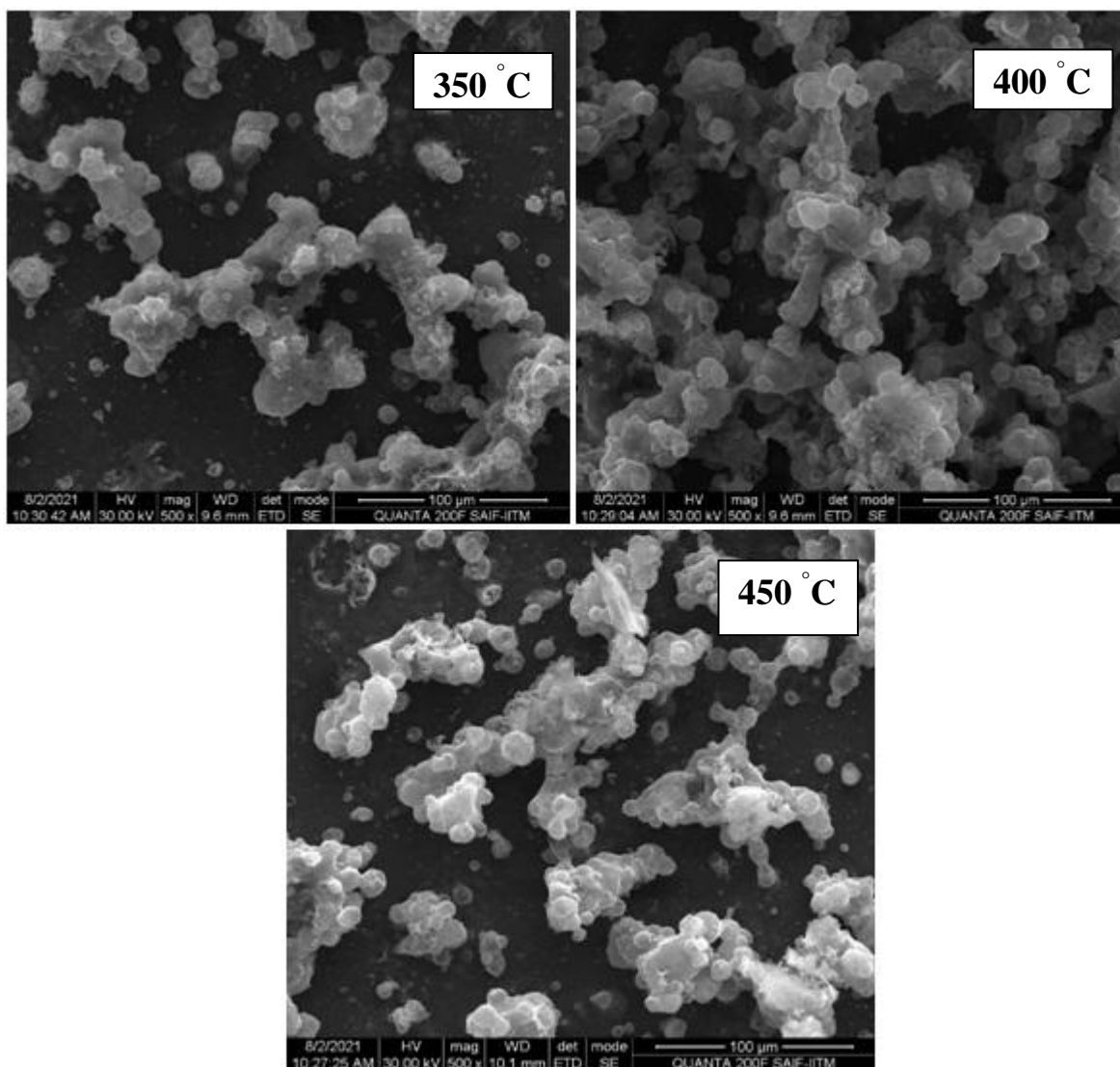


**Fig. 6.** SEM images of prepared  $ZnAl_2O_4$  films at various deposition temperatures

### 3.5 Excitation and Emission Spectrum

The synthesized  $ZnAl_2O_4$  films were tested by fluorescence spectrophotometer to study the luminescence properties. Fig. 7 shows the emission spectra for the excitation wavelength 325 nm. The emission spectra had a broad band between 620 nm and 674 nm. The broad spectrum is due to the different transitions that occurred between the vibrational energy levels. The peaks around 300-350 nm are due to the number of stark levels and the non-removal of degeneracy levels.

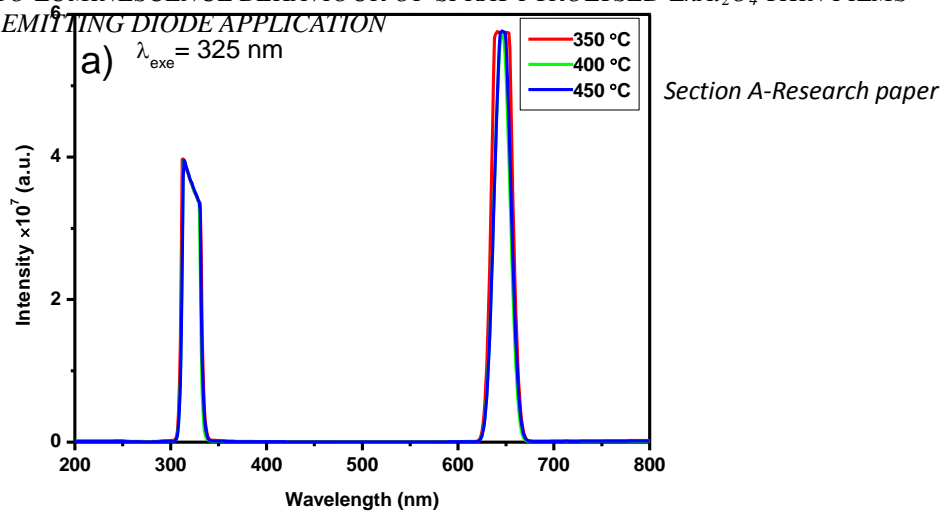


**Fig. 7** Emission spectra of the deposited films excited at 325 nm

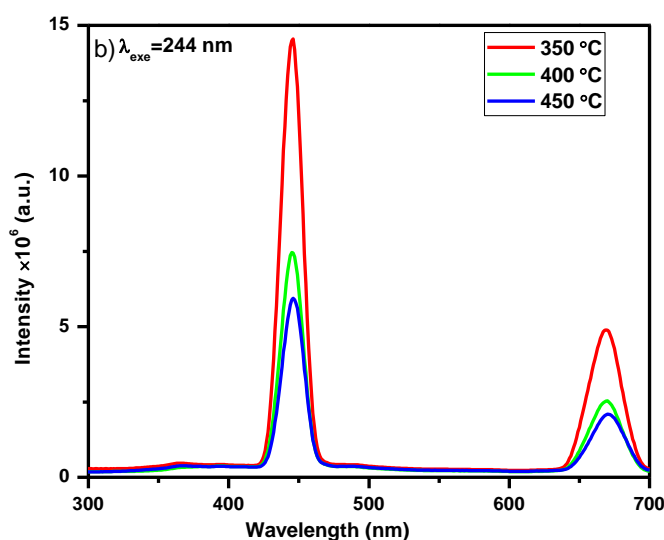


**Fig. 8** Emission spectra of the deposited films excited at 244 nm

According to these results, the emission spectra of 244 nm had two broad bands one located at 445 nm (blue emission), which originated due to the recombination of an electron-hole pair resulting in singly ionized oxygen vacancy-related defects, and the other located at 664 nm (red emission) originated with the oxygen atoms present in the interstitials [31-33].

The PL emission of the ZnAl<sub>2</sub>O<sub>4</sub> films for two different excitations showed a spectrum in the blue and red regions. Moreover, the emission intensity of the synthesized films revealed that the low intensity of emission spectra was due to the separation of charge carriers whereas high intensity confirmed the recombination of charge carriers. Among the four emission bands, the bands located at 646 nm were stronger because the Zn<sup>2+</sup> and Al<sup>3+</sup> ions were located

in the local symmetry environment. Henceforth from the above fact the synthesized  $ZnAl_2O_4$  films deposited at 400 °C were suitable for optoelectronic devices and laser applications.

### 3.6 White light Stimulation

Colour properties of the emitted light from different temperatures were investigated through the chromaticity diagram. Fig. 9 and 10 shows the chromaticity of prepared thin film at the excitation wavelength of 224 nm and 325 nm respectively. The obtained results such as CIE chromaticity colour coordinates (x,y), yellow-to-blue emission intensity ratio (Y/B), and CCT values under various excitations such as 224 nm and 325 nm are tabulated in Table 3.

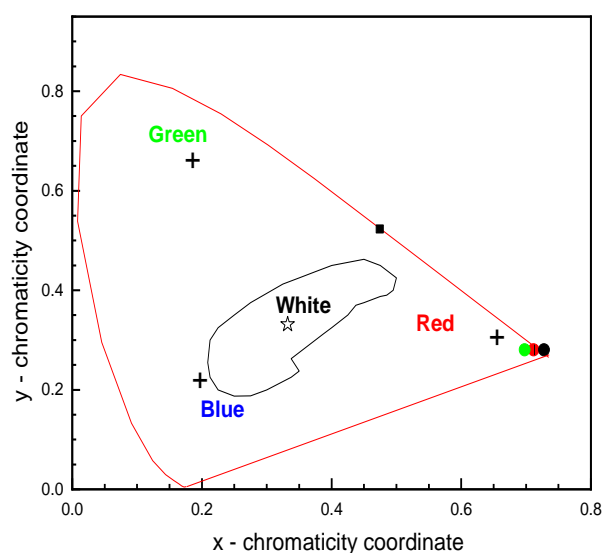


**Fig. 9. CIE Colour Chromaticity diagram of the films corresponding to the excitation Wavelength of 224 nm**

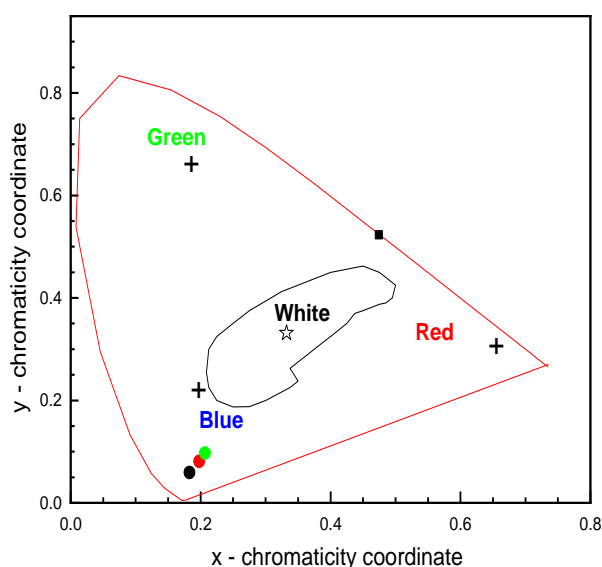


**Fig. 10. CIE Colour Chromaticity diagram of the films corresponding to the excitation wavelength of 325 nm**

**Table 3 Measured Y/B and CCT Values under excitation of 224 nm and 325 nm respectively**

Sample Code	Excitation 224 (nm)				Excitation 325 (nm)			
	X	Y	Y/B	CCT	X	Y	Y/B	CCT
350	0.183	0.059	0.321	1643	0.713	0.280	0.393	5880
400	0.198	0.081	0.409	1620	0.712	0.280	0.394	5886
450	0.207	0.097	0.468	1645	0.713	0.280	0.393	5874

From the results, it was observed that the colour coordinate (x, y) values for the films deposited at various temperature and excited at 224 nm, falls in the blue region on the chromaticity diagram which, concludes the emission of blue light. The colour of the emitting light depended upon the ratio of the intensity of the different emission bands.

By using McCamy's approximation formula given below [34,35]

$$\text{CCT} = -449n^3 + 3525n^2 - 6823.3n + 5520. \quad (4)$$

Here,  $n = (x - x_e)/(y - y_e)$  is the inverse slope line with the epicentre ( $x_e = 0.332$  and  $y_e = 0.186$ ).

The (x,y) coordinates of the prepared films under 224 nm excitation showed a bluish region which was agreeable with the standard value (0.14,0.08). The lesser Y/B ratio indicated a lower degree of covalency in their network. Under 224 nm excitations, all the film deposited at different temperatures emitted dim light (CCT=1640K).

The prepared sample excited at 325 nm, emitted red colour from the chromaticity diagram. Here, the (x,y) coordinates of the prepared film were in good agreement with the standard value (0.67,0.33). Moreover, the prepared film at 325 nm excitation emitted day white light (CCT=5880K) which was higher than the dim light (CCT=1678K). Hence the CCT value under 325 excitation would be larger than the incandescent bulbs, tungsten halogen lamps, and cool white fluorescent lamps.

#### 4. Conclusion

The effect of deposition temperatures on the structural, optical, and photoluminescence properties of spray deposited Zinc Aluminium Oxide films (ZnAl<sub>2</sub>O<sub>4</sub>) were studied. Moreover, the variation of film thickness with substrate temperature was investigated. ZnAl<sub>2</sub>O<sub>4</sub> films deposited at 400 °C exhibited a preferred orientation along the (311) direction and possessed crystalline nature. The emission spectra exhibited blue and red emission under 224 nm and 325 nm excitation respectively. The CCT values confirmed that the synthesized thin film samples could emit warm and cool daylight under different excitation wavelengths. The SEM results revealed porous spherical-shaped particles and the surface microstructure had a dependence on particle substrate temperatures. Thus the synthesized thin film material is very much suitable for the emission of blue light and laser applications.

#### References

- [1] Sea-Fue Wang, Yan-Ting Tsai, Jinn P. Chu, Resistive switching characteristics of a spinel ZnAl<sub>2</sub>O<sub>4</sub> thin film by radio frequency sputtering, *Ceram.Int.*, 42 (2016) 17673-17679
- [2] F.FemilaKomahal, H.Nagabhushana, R.B.Basavaraj, G.P.Darshan, B..Daruka Prasad, Solvothermal synthesis and luminescent properties of hierarchical flowerlike ZnAl<sub>2</sub>O<sub>4</sub>:Ho<sup>3+</sup> microstructures, *Opt. Mater.*, 84 (2018) 536-544.
- [3] Vijay Singha, R.P.S. Chakradharb, J.L. Raoc, Dong-Kuk Kim, Characterization, EPR and luminescence studies of ZnAl<sub>2</sub>O<sub>4</sub>:Mn, *J.Lumin.*, 128 (2008) 394–402.

- [4] M. García-Hipólito, C.D. Hernandez-Perez, O. Alvarez-Fregoso, E. Martinez, J. GuzmanMendoza, C. Falcony, Characterization of europium doped zinc aluminate luminescent coatings synthesized by ultrasonic spray pyrolysis process, *Opt. Mater.* 22 (2003) 345–351.
- [5] H. Zhao, Y. Dong, P. Jiang, G. Wang, J. Zhang, C. Zhang, ZnAl<sub>2</sub>O<sub>4</sub> as a novel high-surface-area ozonation catalyst: One-step green synthesis, catalytic performance and mechanism, *J.Chem.Eng.*, 260 (2015) 623-630.
- [6] P. Mierczynski, W. Maniukiewicz, T.P. Maniecki, Comparative studies of Pd, Ru, Ni, Cu/ZnAl<sub>2</sub>O<sub>4</sub> catalysts for the water gas shift reaction, *Cent. Eur. J. Chem.*, 11 (2013) 912-919.
- [7] E.L. Foletto, S. Battiston, J.M. Simoes, M.M. Bassaco, L.S. Fagundes Pereira, E.M. M. Flores, E.I. Muller, Synthesis of ZnAl<sub>2</sub>O<sub>4</sub> nanoparticles by different routes and the effect of its pore size on the photocatalytic process, *Micr. Meso.Mater.* 163 (2012) 29-33.
- [8] M. Shahmirzaee, M. Shafiee Afarani, A. Masoud Arabi, A. IranNejhad, In situ crystallization of ZnAl<sub>2</sub>O<sub>4</sub>/ZnO nanocomposite on alumina granule for photocatalytic purification of wastewater, *Res.Chem.Intermed.*, 43 (2017) 321-340.
- [9] X. Yuan, X. Cheng, Q. Jing, J. Niu, D. peng, Z. Feng and X. Wu, ZnO/ZnAl<sub>2</sub>O<sub>4</sub> Nanocomposite with 3D Sphere -Like Hierarchical Structure for Photocatalytic Reduction of Aqueous Cr(VI), *Mater.*, 11(2018) 1624-1647.
- [10] XinYong Li, ZhengruZhua, QidongZhaoa, Lianzhou Wang, Photocatalytic degradation of gaseous toluene over ZnAl<sub>2</sub>O<sub>4</sub> prepared by different methods: A comparative study, *J. Hazard. Mater.*, 186 (2011) 2089–2096
- [11] Chong Peng, Guogang Li, DonglingGeng, Mengmeng Shang, Zhiyao Hou, Jun Lin, Fabrication and luminescence properties of one-dimensional ZnAl<sub>2</sub>O<sub>4</sub> and ZnAl<sub>2</sub>O<sub>4</sub>: A<sup>3+</sup> (A = Cr, Eu, Tb) microfibers by electrospinning method, *Mater.Res.Bull.*, 47 (2012) 3592-3599.
- [12] BaochangChengn, Zhiyong Ouyang, Baixiang Tian, Yanhe Xiao, Shuijin Lei, Poros ZnAl<sub>2</sub>O<sub>4</sub> spinel nanorods: high sensitivity humidity sensors. *Ceram.Int.*, 39 (2013) 7379–7386.
- [13] Zhengru Zhu, Qidong Zhao, Xinyong Li, Hong Li, ac Moses Tade and Shaomin Liu, Photocatalytic performances and activities in Ag-doped ZnAl<sub>2</sub>O<sub>4</sub> nanorods studied by FTIR spectroscopy, *Catal.Sci.Techno.*, 3 (2013) 788—796.
- [14] Yang Yang, Dong Sik Kim, Roland Scholz, Mato Knez, Seung Mo Lee, Ulrich Gose le, and Margit Zacharias, Hierarchical three-dimensional ZnO and their shape-preserving transformation into hollow ZnAl<sub>2</sub>O<sub>4</sub> nanostructures, *Chem.Mater.*, 20 (2008) 3487–3494.



- [15] Lu Zou, Feng Li, Xu Xiang, David G. Evans, and Xue Duan, Self-generated template pathway to high-surface-area zinc aluminate spinel with mesopore network from a single-source inorganic precursor, *Chem.Mater.*, 18 (2006) 5852–5859.
- [16] Yiquan Wu, Jing Du, Kwang-Leong Choy, Larry L. Hench, Jingkun Guo, Formation of interconnected microstructural ZnAl<sub>2</sub>O<sub>4</sub> films prepared by sol-gel method, *Thin Solid Films*, 472 (2005) 150 – 156.
- [17] Gurpreet Kaur, Anirban Mitra, K.L. Yadav, Pulsed laser deposited Al-doped ZnO thin films for optical applications, *Progress in Natural Science: Materials International*. 25 (2015) 12-21.
- [18] S.P. Khambule, S.V. Motlounge, T.E. Motaung, L.F. Koao, R.E. Kroon g, M.A. Malimabe, Tuneable blue to orange phosphor from Sm<sup>3+</sup> doped ZnAl<sub>2</sub>O<sub>4</sub> nanomaterials *J.Opt.*, 9( 2022) 100280.
- [19] W.Siefert, Properties of thin In<sub>2</sub>O<sub>3</sub> and SnO<sub>2</sub> films prepared by corona spray pyrolysis and a discussion of the spray pyrolysis process, *Thin Solid Films*, 121 (1984) 275-282
- [20] Lado Filipovic, Siegfried Selberherr, Giorgio C. Mutinati, F. Schrank, Methods of stimulating Thin Film Deposition using spray pyrolysis techniques, *Microelectron. Eng.*, 117 (2014) 57-66.
- [21] A. Bouhemadou, R. Khenata, Pseudo-potential calculations of structural and elastic properties of spinel oxides ZnX<sub>2</sub>O<sub>4</sub> (X = Al, Ga, In) under pressure effect, *Phys.Lett.A.*, 360 (2006) 339-343.
- [22] Sabrina Iaiche, Chahra Boukaous, David Alamarguy, Abdelkadar Djelloul, and Djamel Hamana, Effect of Solution Concentration on ZnO/ZnAl<sub>2</sub>O<sub>4</sub> Nanocomposite Thin Films Formation Deposited by Ultrasonic Spray Pyrolysis on Glass and Si (111) Substrates. *J.Nano.Res.*, 63 (2020) 10-30.
- [23] S.Y. Hu, Y.C. Lee, J.W. Lee, J.C. Huang, J.L. Shen, W. Water, The Structural and Optical Properties of ZnO/Si thin films by RTA treatments, *App.Sur.Sci.*, 254 (2008) 1578-1582.
- [24] M.F. Malek, M.H. Mamat, M.Z. Musa, Z. Khusaimi, M.Z. Sahdan, A.b. Suriani, A. Ishak, I. Saurdi, R. Mohamed, M. Rusop, Thermal annealing of – induced formation of ZnO nanoparticles: Minimum stress and strain ameliorate preferred c-axis orientation and crystal growth properties, *J.Alloys.Comp.*, 610 (2014) 575-588.
- [25] A. Moses Ezhil Raj, K.C. Lalithambika, V.S. Vidhya, G. Rajagopal, A. Thayumanavum, M. Jayachandran, C. Sanjeeviraja, Growth mechanism and Optoelectronic properties of

nanocrystalline In<sub>2</sub>O<sub>3</sub> films prepared by Chemical Spray pyrolysis of metal-organic precursor, *Physics B.*, 403 (2008) 544-554.

[26] M. Kumar, V. Natarajan and S.V Godbole, Synthesis, characterization, photoluminescence and thermally stimulated luminescence investigations of orange red-emitting Sm<sup>3+</sup> doped ZnAl<sub>2</sub>O<sub>4</sub> phosphor, *Bull. Mater. Sci.*, 37 (2014) 1205–1214.

[27] K. Bouzid, A. Djelloul, N. Bouzid, J. Bougdira, Electrical resistivity and photoluminescence of zinc oxide films prepared by ultrasonic spray pyrolysis, *Phys.Stat. Sol. A*, 206: 1 (2009) 106–115.

[28] Nabeel A Bakri, A.M. Fundei, V.S.Wamani, M.M.Kamblei, R. R.Rhawaldar, D.P. Amalnerkar, S.W.Gosavi and S.R.Jadkar, Determination of the optical parameters of a-Si: H thin films deposited by hot wire–chemical vapor deposition technique using transmission spectrum only, *J. Phy* 76: (2011) 519-531.

[29] N.M. Ravindra, Preethi Ganapathy, Jinsoo Choi, Energy gap–refractive index relations in semiconductors – An overview, *Infrared.Phys.Techno.*, 50 (2007) 21–29

[30] G.Koretchenkov, V. Brinzari, M. Ivanov, A.Cerneavschi, J.Rodriguez, A.Cirere, A.Cornet, J.Morante, Structural Stability of In<sub>2</sub>O<sub>3</sub> films deposited by spray pyrolysis during thermal annealing, *Thin Solid Films*, 479 (2005) 38-51.

[31] M.A. Lahmer, First-principles study of the structural, electronic, and optical properties of the clean and O-deficient ZnAl<sub>2</sub>O<sub>4</sub>(110) surfaces *Surf.Sci.*, 677 (2018) 105-114.

[32] S.V. Motlounge, K.G. Tshabalala, R.E. Kroon, T.T. Hlatshwayo, M. Mlambo, S. Mpelane, Effect of Tb<sup>3+</sup> concentration on the structure and optical properties of triply doped ZnAl<sub>2</sub>O<sub>4</sub>: Ce<sup>3+</sup>, Eu<sup>3+</sup>, Tb<sup>3+</sup> nano-phosphors synthesized via citrate sol-gel method, *J. Mol.Struct.*, 1175 (2019) 241-252.

[33] L.F. Koao, B.F. Dejene, F.G. Hone, H.C. Swart, S.V. Motlounge, T.E. Motaung, V.B. Parade, Effects of octadecyl amine molar concentration on the structure, morphology and optical properties of ZnO nanostructure prepared by homogeneous precipitation method, *J.Lumin.*, 200 (2018) 206-215.

[34] S.A. Azizan, S. Hashim, N.A. Razak, M.H.A. Mhareb, Y.S.M. Alajerami, N. Tamchek, Physical and optical properties of Dy<sup>3+</sup>: Li<sub>2</sub>O-K<sub>2</sub>O-B<sub>2</sub>O<sub>3</sub> glasses, *J. Mol. Struct.* 1076 (2014) 20–25.

[35] Manjeet, A. Kumar, Anu, Ravina, Nisha Deopa, Anand Kumar, R.P. Chahal, S. Dahiya, R. Punia, A.S. Rao, Structural, thermal, optical and luminescence properties of Dy<sup>3+</sup> ions doped Zinc Potassium Alumino Borate glasses for optoelectronics applications, *J.Non.Cryst.Solids.*, 588 (2022) 121613.